comments and aid in preparing the manuscript are gratefully acknowledged. Useful comments of a referee are also deeply appreciated.

References and Notes

(1) See, for example: Kurata, M.; Tsunashima, Y.; Iwama, M.; Kamada, K. In *Polymer Handbook*; Brandrup, J., Immergut, E. H., Eds.; Wiley Interscience: New York, 1975.
(2) Einaga, Y.; Miyaki, Y.; Fujita, H. *J. Polym. Sci., Polym. Phys. Ed.* **1979**, *17*, 2103.
(3) Miyaki, Y. Ph.D. Thesis, Osaka University, Osaka, Japan, 1981.
(4) Meyerhoff, G.; Appelt, B. *Macromolecules* **1979**, *12*, 968.
(5) Kirkwood, J. G.; Riseman, J. *J. Chem. Phys.* **1948**, *16*, 67.
(6) Kirkwood, J. G. *J. Polym. Sci.* **1954**, *12*, 1.
(7) Debye, P.; Bueche, A. M. *J. Chem. Phys.* **1948**, *16*, 573.
(8) Kuhn, W. *Kolloid Z.* **1934**, *68*, 2.
(9) Flory, P. J. *J. Chem. Phys.* **1949**, *17*, 303; *Principles of Polymer Chemistry*; Cornell University Press: Ithaca, NY, 1953.
(10) Yamakawa, H.; Fujii, M. *Macromolecules* **1974**, *7*, 128.
(11) Oono, Y.; Kohmoto, M. *J. Chem. Phys.* **1983**, *78*, 520. Oono, Y. *Adv. Chem. Phys.* **1985**, *61*, 301. Douglas, J. F.; Freed, K. F. *Macromolecules* **1984**, *17*, 2344; **1985**, *18*, 201.
(12) Kashiwagi, Y.; Einaga, Y.; Fujita, H. *Polym. J.* **1980**, *12*, 271.
(13) Wang, S.-Q.; Douglas, J. F.; Freed, K. F. *Macromolecules* **1985**, *18*, 2464.
(14) Miyaki, Y.; Fujita, H.; Fukuda, M. *Macromolecules* **1980**, *13*, 588.
(15) Schmidt, M.; Burchard, W. *Macromolecules* **1981**, *14*, 210.
(16) Tsunashima, Y.; Nemoto, N.; Kurata, M. *Macromolecules* **1983**, *16*, 1184.
(17) ter Meer, H.-U.; Burchard, W. *Colloid Polym. Sci.* **1980**, *258*, 675.
(18) Mandelkern, L.; Flory, P. J. *J. Am. Chem. Soc.* **1952**, *74*, 2517.
(19) Klaerner, P. E. O.; Ende, H. A. In *Polymer Handbook*; Brandrup, J., Immergut, E. H., Eds.; Wiley Interscience: New York, 1975.
(20) Yamakawa, H. *Modern Theory of Polymer Solutions*; Harper & Row: New York, 1971.
(21) Wang, S.-Q.; Douglas, J. F.; Freed, K. F. *J. Chem. Phys.* **1986**, *85*, 3674.
(22) Zimm, B. H. *Macromolecules* **1980**, *13*, 592.
(23) Garcia de la Torre, J.; Jimenez, A.; Freire, J. J. *Macromolecules* **1982**, *15*, 148.
(24) Fixman, M. *Macromolecules* **1981**, *14*, 1710.
(25) Bruns, W. *Macromolecules* **1984**, *17*, 2826.
(26) Cherayil, B. J.; Douglas, J. F.; Freed, K. F. *J. Chem. Phys.* **1985**, *83*, 5293.
(27) Fujita, H.; Norisuye, T. *Macromolecules* **1985**, *18*, 1637.
(28) Tong, Z.; Ohashi, S.; Einaga, Y.; Fujita, H. *Polym. J.* **1983**, *15*, 835. Takano, N.; Einaga, Y.; Fujita, H. *Polym. J.* **1985**, *17*, 1123.
(29) Perzynski, R.; Delsanti, M.; Adam, M. *J. Phys.* **1987**, *48*, 115.
(30) Gobush, W.; Solc, K.; Stockmayer, W. H. *J. Chem. Phys.* **1974**, *60*, 12.
(31) Tanaka, G.; Solc, K. *Macromolecules* **1982**, *15*, 791.
(32) Barrett, A. J. *Macromolecules* **1985**, *18*, 196.
(33) Burch, D. J.; Moore, M. A. *J. Phys. A: Math. Gen.* **1976**, *9*, 435.
(34) Elderfield, D. J. *J. Phys. A: Math. Gen.* **1978**, *11*, 2483; *J. Phys. C* **1980**, *13*, 5883.
(35) des Cloizeaux, J. *J. Phys. (Les Ulis, Fr.)* **1981**, *42*, 635.
(36) Oono, Y.; Freed, K. F. *J. Phys. A: Math. Gen.* **1982**, *15*, 1931.
(37) Douglas, J. F.; Freed, K. F. *Macromolecules* **1984**, *17*, 1854.
(38) Miyaki, Y.; Einaga, Y.; Fujita, H. *Macromolecules* **1978**, *11*, 1180. Hirosye, T.; Einaga, Y.; Fujita, H. *Polym. J.* **1979**, *11*, 819.
(39) Huber, K.; Bantle, S.; Lutz, P.; Burchard, W. *Macromolecules* **1985**, *18*, 1461.
(40) Huber, K.; Stockmayer, W. H. *Macromolecules* **1987**, *20*, 1400.
(41) Norisuye, T.; Fujita, H. *Polym. J.* **1982**, *14*, 143.
(42) Benoit, H.; Doty, P. *J. Phys. Chem.* **1953**, *57*, 958.
(43) Kratky, O.; Porod, G. *Recl. Trav. Chim., Pay-Bas* **1949**, *68*, 1106.
(44) Yamakawa, H.; Stockmayer, W. H. *J. Chem. Phys.* **1972**, *57*, 2843.
(45) Yamakawa, H.; Shimada, J. *J. Chem. Phys.* **1985**, *83*, 2607.
(46) Murakami, H.; Norisuye, T.; Fujita, H. *Macromolecules* **1980**, *13*, 345.

Zigzag Polyamides Comprising Rodlike Segments Connected by Freely Rotating or Stiff Joints

Shaul M. Aharoni

Allied-Signal Corporation, Engineered Materials Sector Laboratories, Morristown, New Jersey 07960. *Received April 17, 1987; Revised Manuscript Received June 22, 1987*

ABSTRACT: Six fully aromatic zigzag polyamides were synthesized and characterized. The angles between their rigid rodlike segments are all fixed at 119° and 120°. Three of the polyamides have joints between the rodlike segments with free torsional rotation, and three have rather stiff joints. In solution and the amorphous bulk they all adopt a random coil configuration. The behavior of all polymers in dilute solution is dictated by their equilibrium rigidity, with no significant difference between those having freely rotating joints and those having stiff joints. With increased concentration effects of kinetic rigidity become more prominent because the slowness or rapidity of torsional motion interferes in varying degrees with the free movement of interpenetrated coils and their segments. Two groups of radii of gyration were measured in dilute solution for all polymers. The large R_G's are a measure of the coil dimensions, while the smaller R_G's and the hydrodynamic radius reflect the fact that in coils with long rodlike segments only a small fraction of the solvent in the volume pervaded by the coil is actually interacted with the coil and hydrodynamically affected by its presence.

Introduction

In this paper solution properties of six fully aromatic polyamides will be described. Each of these polymers comprises rodlike segments of identical length connected to one another by joints having either high degree or low degree of torsional mobility. When the chains of the six polyamides are fully extended in a plane, they appear as long zigzags and hence their name. The six polyamides are divided into two groups. One includes three polyamides whose joints are essentially freely rotating. These polymers were briefly described recently.[1] The second group contains three additional zigzag polyamides whose joints are substantially stiffer, severely reducing the torsional rotation freedom of their rodlike segments.

The behavior of the zigzag polyamides in dilute and concentrated solutions appears to be controlled by two important structural features. The first is the length l_o of the rodlike segments characteristic of each polymer. In our case this length corresponds to the length of the average virtual bond of the polymer. The second feature is the degree of freedom for torsional rotation around the joints connecting these segments. These two structural

0024-9297/88/2221-0185$01.50/0

features are conveniently described in terms of the Soviet school of Tsvetkov and associates.[2-5] Accordingly, the equilibrium rigidity of polymeric chains depends on l_0 and characterizes the average macromolecular conformation at equilibrium in dilute solution. The length of the Kuhn segment, A, the chain persistence length, $q = A/2$, and the chain's radius of gyration, R_G, are all quantitative reflections of the equilibrium chain rigidity. The kinetic rigidity characterizes the kinetics of conformational change of a macromolecule in terms of the time required for the chain to change from one conformation to another. High kinetic rigidity means that the molecule retains its conformation unchanged during a fairly long period of time.[3] In terms of the rotational isomers model, the equilibrium rigidity is reflected by the average chain dimensions, while the kinetic rigidity is a reflection of the hinderance to change from one isomeric state to another.

For a randomly coiled polymer with a fixed contour length, L, the end-to-end distance, the radius of gyration, and the volume pervaded by the coil are directly related to the length l_0 of an actual or virtual bond along the chain. This means that in dilute solution the average distance between unjoined segments of the chain is linearly dependent on their length. Therefore, the segmental length affects the chain behavior in dilute solution in two ways. The first is the well-established increase in coil volume as a function of l_0. The second way is the decrease in the volume fraction of solvent molecules entrained by the coil relative to the volume pervaded by it: once the distance between one rodlike segment and others becomes much larger than the average size of solvent molecules, a decreasing fraction of the solvent molecules in the pervaded volume are affected by the macromolecular chain to such an extent as to be attached to it and entrained by it. Solvent molecules form a dynamic sheath around the coiled chain, but most solvent molecules within the volume encompassed by the chain are not affected by or recognize its presence. At constant L the fraction of solvent molecules from the pervaded volume interacting with the coil decreases with increase in l_0. In most coiled molecules the effects of l_0 are noticed only inasmuch as they affect the coil size simply because l_0 is usually smaller than or about equal to the size of solvent molecules.

In our previous paper on zigzag polymers,[1] the poly(ester amides) exhibited weak interactions with the solvent and were described in terms of partly draining coils, while the polyamides strongly interact with the solvent and were described in terms of nondraining coils. In this paper the nondraining model for zigzag polyamides is refined to take account of both the effects of the length l_0 and the kinetic rigidity of the chain.

The behavior of poly(*m*-phenylene isophthalamide) (PPI) and poly(aryl ether ketone) (PEEK) in the bulk and especially in solution is highly instructive because of the gross similarity of these polymers to our zigzag polyamides. Both PPI and PEEK can be visualized as zigzag polymers with rather short l_0. In the case of PEEK the ether oxygen allows for a substantially free rotation while the ketone group is somewhat more restrictive. In the case of PPI the meta placement of bonds greatly increases the kinetic rigidity of the chain. In both instances the chain adopts the configuration of a random coil and is not extended in space in the form of a planar zigzag. The Kuhn segment length and the number of repeat units per Kuhn segment, A/l_0, for both PEEK and PPI reflect chains with equilibrium rigidity far smaller than for rodlike molecules such as poly(*p*-benzamide) (*p*-BA) or poly(*p*-phenylene terephthalamide) (PPT) but significantly larger than for common flexible chain polymers. Thus, for PEEK[6] A = 108 Å and A/l_0 = 19.4. For PPI, A = 50 Å[2] or 45 Å[7] or 34 ± 5 Å,[8] depending on the solvent, and A/l_0 = 8.4[2] or 7.5.[3] These values are far smaller than A = 2100 Å for *p*-BA and A = 1300 Å for PPT in concentrated H_2SO_4 and A/l_0 values both in the hundreds.[2] Reflecting the strong dependence of A on l_0, the values of A for PEEK and PPI are substantially larger than the values for common flexible polymers,[9] but the ratios A/l_0 remain relatively small, similar to those obtained from common flexible coils.

In the bulk both PEEK[6] and PPI[10] are highly crystalline, with even the supposedly less flexible PPI showing around 50% crystallinity. The amorphous and crystalline densities of PPI[10] and PEEK[11] are very similar to those of poly(ethylene terphthalate),[12] indicating that possible rotational restrictions imposed by the meta-substituted rings in the PPI pose no significant hinderance to chain packing in both the amorphous and crystalline phases.

In our case changes in the equilibrium rigidity were effected by changing the length l_0 of the rodlike segments, and changes in the kinetic rigidity were made by changing the joints between them from the freely rotating ether oxygen with low kinetic rigidity to the meta-substituted aromatic ring, a stiff joint with high kinetic rigidity. The solution properties of zigzag polyamides will be evaluated first in terms of equilibrium rigidity and draining effects and then in terms of the different kinetic rigidity of polymers with freely rotating and stiff joints.

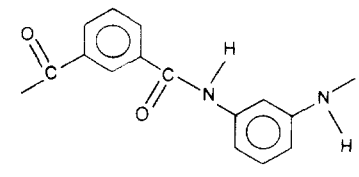

PPI

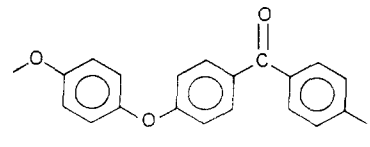

PEEK

Experimental Section

(a) Synthesis. All polymerizations were carried out at about 100 °C in 5% wt/vol % solutions of LiCl in *N,N*-dimethylacetamide (DMAc/5% LiCl) in the presence of pyridine and triphenyl phosphite.[13,14] The monomer charge was about 10% based on the combined volume of the solvent and liquid reagents. The polymerizations were usually continued for 3 h, yielding essentially quantitative yields.[14] After precipitation in excess methanol, the polymers were washed in water, water/methanol, and methanol and finally dried to cosntant weight in a vacuum oven at >100 °C. By the correct choice of diamine and dicarboxyl monomers, polymers with identical repeat units were obtained in each polymerization run. Specifically, the polyamide **1a** (see below) was prepared from equimolar amounts of 4,4′-dicarboxydiphenyl ether and 4-aminophenyl ether, the polyamide **1b** from 4,4′-dicarboxydiphenyl ether and *p*-phenylenediamine, and **1c** from 4,4′-dicarboxydiphenyl ether and 4,4-diaminobenzanilide. Polymer **14C** was made from isophthalic acid and 4,4′-diaminobenzanilide. For preparation of polyamide **14D**, the monomer *p*-dicarboxyphenylene isophthalamide was prepared by a Schotten–Baumann procedure from isophthaloyl chloride and *p*-aminobenzoic acid in 1:2 molar ratio. This monomer was purified and subsequently reacted under Yamazaki conditions[13,14] with 4,4′-diaminobenzanilide to produce the desired polymer. For polyamide **14B**, the monomer 4,4′-diaminobenzanilide isophthalamide was prepared under Schotten–Baumann conditions from isophthaloyl chloride and a tenfold molar excess of 4,4′-diaminobenzanilide. After purification, this monomer was reacted with terephthalic acid under Yamazaki conditions to produce polyamide **14B**.

The monomer 4,4′-diaminobenzanilide was obtained from Sandoz Corp. and recrystallized from 10:1 methanol/acetone at least twice prior to use. 4,4′-dicarboxydiphenyl ether was acquired from Chem Service Co., and used as is. All other monomers, reagents, and solvents were obtained from chemical supply houses and used as received.

(b) Characterization. The structures of all polymers and monomeric intermediates prepared in this study were confirmed by carbon-13 NMR spectra obtained with a Varian XL-200 Fourier transform NMR spectrometer from solutions in deuteriated DMAc. Crystallinity indices of all polyamides were estimated from wide angle X-ray diffraction (WAXD) patterns obtained from the powdered polymers in a Philips diffractometer operating in parafocus mode with monochromatized copper Kα radiation. Infrared scans were obtained from the pulverized polymers in KBr pellets with a Perkin-Elmer Model 283B infrared spectrometer. The densities of the zigzag polyamides were measured by pycnometry as described in ref 1.

All viscosities were measured at 25 °C in DMAc/5% LiCl solutions. Intrinsic viscosities were measured in internal dilution glass viscometers with solvent flow time of not less than 100 s. The solution flow rate in the glass viscometers was sufficiently slow for the measured viscosities to approach η_o, the zero shear viscosity. The solvent viscosity, η_s, of DMAc/5% LiCl at 25 °C was measured with calibrated glass viscometers and with a Nametre direct readout viscometer and was found to be 2.39 ± 0.05 cP (centipoises). High concentration viscosities were measured in large bore glass viscometers and with the Nametre direct readout viscometer. The viscosities (in centipoise) obtained by both procedures were very close to one another. The solution flow time in the large bore glass vicometers was in the range of 500 to over 1000 s.

For all light scattering work, at least four different concentrations of each polyamide in DMAc/5% LiCl were prepared and filtered with Millex filter units (0.2 μm pore diameter) from Millipore. Weight average molecular weight, M_w, was measured by low-angle laser light scattering using a Chromatix KMX-6 instrument, on solutions spanning the range of 1.0–0.2% concentration. In this case no aggregation effects were noticed. The error margin for the M_w determinations was ±3% or less. It should be borne in mind that this error estimate carries over to all molecular dimensions obtained from M_w.

Depolarization ratios, ρ, were measured in a Langley–Ford multiangle photon correlation instrument Model LSA II, equipped with a polarizer at each of the seven angles of measurement. Each angle, θ, ranging from about 10° to 152°, was calibrated for absolute Rayleigh ratio measurements by measuring the light scattering intensity of pure toluene, a solvent with a known Rayleigh ratio. The depolarization ratio is the ratio of the horizontally polarized to vertically polarized intensities (after subtracting the corresponding values for the solvent), which were measured at each of the seven scattering angles. For these measurements, four concentrations of each polyamide in DMAc/5% LiCl in the interval of 1.0–0.4% were measured, but the resulting depolarization ratios appeared to be insensitive to changes in concentration.

Now, it has been shown by Benoit and Doty[15] that for a wormlike chain of contour length, L, the radius of gyration, R_{Gw}, can be obtained from the relationship

$$R_{Gw} = q[x/3 - 1 + 2/x + 2(1 - e^{-x})/x^2]^{1/2} \quad (1a)$$

where $x = L/q$. The optical anisotropy Δ^2 for such a chain was calculated[16] to be

$$\Delta^2 = \delta_0^2[2/x' - 2(1 - e^{-x'})/x'^2] \quad (2)$$

where $x' = 3L/q$ and δ_0^2 is the optical anisotropy for the structural segment. The values of δ_0^2 are usually obtained by extrapolation of the values of Δ^2 determined for chains of decreasing length to their values at $N = 1$:

$$\delta_0^2 = \Delta^2 \qquad (N = 1) \quad (3)$$

In our case N is the weight average number of rodlike segments in the chain. The optical anisotropy Δ^2 is calculated from the measured depolarization ratio, ρ. The relationship between Δ^2 and ρ depends on the nature of the incident light. In the case of unpolarized incident light, the depolarization ratio ρ_u at a scattering angle, $\theta = 0°$, relates to Δ^2 as[16,17]

$$\Delta^2 = 5\rho_u/(6 - 7\rho_u) \quad (4)$$

but in the case of vertically polarized incident light[18] at $\theta = 0°$

$$\Delta^2 = 5\rho_v/(3 - 4\rho_v) \quad (5)$$

In our case, vertically polarized incident light was used. Data were collected at seven scattering angles and corrected to zero angle by the use of the equation

$$\rho_v = \rho_\theta(1 + \cos^2\theta)/[2 - \rho_\theta(1 - \cos^2\theta)] \quad (6)$$

Persistence lengths and radii of gyration are obtainable, hence, from measurements of depolarization ratios of scattered light, provided L is known. As we had at our disposal a series of monodisperse oligomers of rodlike aromatic polyamides[19] essentially identical in composition to the present rodlike chain segments, we measured their optical anisotropies, Δ^2, in DMAc/5% LiCl and used these values to accurately determine the values of δ_0^2 and magnitudes of the radii of gyration obtained from depolarization measurements, R_{Gdep}, for the polymers in this study. It was previously found that in the case of rodlike polyamides with relatively low polydispersity, the measured values of ρ_v and the resulting q appear to be independent from such polydispersity.[19] Because of the similar polymerization procedures, this independence most likely carries over to systems such as the present.

Hydrodynamic radii, R_H, were determined from diffusion coefficients, D, measured by photon correlation spectroscopy (PCS) in the LSA II multiangle photon correlation instrument. Solutions in DMAc/5% LiCl of at least four different concentrations within the range of 1.0–0.4% were prepared from each polyamide and both centrifuged and filtered as specified above. Ideally, analysis should be performed on "perfect" data, i.e., no dust or aggregates in the solution. Unfortunately, despite repeated filtering and centrifugation (the most successful combination), no such perfection was obtained, presumably due to reformation of aggregates. Thus, we were reduced to making the best of a bad situation. First, we took at least ten data sets at each concentration and angle and rejected most of them on the basis of a simple linearized cumulant fit (abnormally high base lines, large particle sizes, etc.); basically, the sets that gave the smallest polymer size and the lowest base line were retained. At times, all the sets were rejected and the measurement was repeated on new solutions. When reasonably "clean" correlation functions were obtained, with consistent sizes and base lines, the data analysis was continued by using two different methods. First, a more elaborate nonlinear cumulant fit was used, emphasizing the beginning of the correlation function. The second algorithm was DISCRETE, a nonlinear multiexponential fitting routine, where the fastest exponential obtained was taken to correspond with the nonaggregated polymer. Both methods yielded similar results. However, DISCRETE was found to yield more consistent results, i.e., data on the same polymer at different angles and/or levels of cleanliness were more likely to give the same diffusion coefficient D. Again, failure to give such consistency resulted in the rejection of the data and the repeat of the measurements on fresh solutions. The measured diffusion coefficients were extrapolated to zero concentration before the value of R_H was calculated from

$$R_H = kT/6\pi\eta_s D \quad (7)$$

where k is the Boltzmann constant, T is the absolute temperature, η_s is the solvent viscosity, 0.0239 P in our case, and D is the diffusion coefficient in cm^2/s.

Light scattering dissymmetry results were in qualitative agreement with the results obtained from depolarization ratios. However, the wide scatter in the dissymmetry measurements prevented a reasonable quantitative agreement, compelling us to abandon the dissymetry results.

Results

The identical rodlike segments of each aromatic zigzag polyamide, together with their joints at both ends, are shown in Chart I. In polymers **1a**, **1b**, and **1c**, the joints consist of a single oxygen atom, allowing for essentially free

Chart I

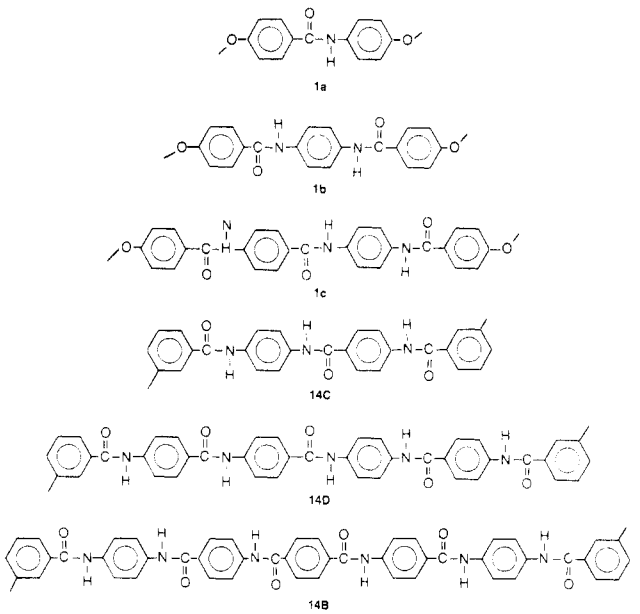

torsional rotation[20] of the rodlike segments. The long rodlike segments of the other three polyamides, namely, **14C**, **14D**, and **14B**, are connected to one another by an isophthaloyl residue, maintaining an angle of $\theta = 120°$ between adjoining segments and restraining their torsional rotation. The length l_o of the rodlike segments (i.e., virtual bonds), the angle θ between the freely rotating ones, and the projected bond length $l_o \sin(\theta/2)$ were calculated from data of Tonelli[20,21] and Flory and associates.[22,23] By definition, the chain contour length L is Nl_o and the chain end-to-end distance, L_w, is $Nl_o \sin(\theta/2)$.

Estimates of the radius of gyration, R_G, are available from several theoretical models. For the classical Gaussian freely jointed chains[24]

$$R_{Gg} = l_o(N/6)^{1/2} \tag{8}$$

and for the freely rotating chain of large N and a single fixed angle, θ, the radius of gyration is

$$R_{Gfr} = [(N/6)l_o^2(1 - \cos\theta)/(1 + \cos\theta)]^{1/2} \tag{9a}$$

$$R_{Gfr} = R_{Gg}[(1 - \cos\theta)/(1 + \cos\theta)]^{1/2} \tag{9b}$$

In our case the fixed angles between the virtual bonds are 119° for the ether joints[20,21] and 120° for the isophthalamide group, placing the values of R_{Gfr} in the narrow range of $1.70R_{Gg} \leq R_{Gfr} \leq 1.73R_{Gg}$.

According to Benoit and Doty[15] and Yamakawa,[25] the radius of gyration of the wormlike chain, R_{Gw}, is obtained from

$$R_{Gw} = [(Lq/3) - q^2 + (2q^3/L) - (2q^4/L^2)(1 - e^{-L/q})]^{1/2} \tag{1b}$$

where q is the chain's persistence length, equalling half its Kuhn segment length, A. For chains with $L/q \gg 1$, the general relationship[26]

$$6R_G/L = 2q[1 - (L/q)^{-1}] \tag{10}$$

holds, and from this one obtains the approximation

$$A = 2q \cong 6R_G^2/L \tag{11}$$

Experimental estimates of the radius of gyration are obtained from measurements of $[\eta]$, the intrinsic viscosity

$$R_{Gvisc} = ([\eta]M/6^{3/2}\phi_\infty)^{1/3} \tag{12}$$

where M is the molecular weight and $\phi_\infty = 2.68 \times 10^{21}$ when the viscosity is measured in units of dL/g.[27] Tanford[28] showed that the radius of gyration for freely draining coils, R_{Gfd}, can be closely approximated from measured values of M, $[\eta]$, and the radius of the hydrodynamically equivalent sphere R_H

$$R_{Gfd} = (M[\eta]/\pi N_a R_H)^{1/2} \tag{13}$$

where N_a is Avogadro's number. The radius of gyration for nondraining coils, R_{Gnd}, can be approximated from R_{Gfd} by the use of the relationship[28]

$$R_{Gnd} = R_{Gfd}/(3.3)^{1/2} \tag{14}$$

The four experimental radii above, namely, R_H, R_{Gvisc}, R_{Gfd}, and R_{Gnd}, reflect the hydrodynamic and thermodynamic interactions between the polymer chain and solvent molecules in which it is immersed. That is, these radii reflect the amount of solvent molecules entrained by the polymeric coil and attracted to it to such an extent that their motional freedom is substantially affected by the movement of the polymer chain in the solvent. Other methods are not sensitive to the hydrodynamic interactions of polymer coils and, hence, may produce characteristic sizes different from the radii above. One such method measures the ratios of the intensities of scattered depolarized light, as described above.

Table I
Calculated Radii of Gyration Based on Freely Jointed and Freely Rotating Models[a]

polymer code	M_w	l_o	N	L_w	R_{Gg}	R_{Gfr}
			Freely Rotating Joints			
1a	24000	10.64	114	1050	46.4	78.7
1b	18000	17.14	55	810	51.9	89.9
1c	22000	23.64	49	1000	67.6	117.1
			Stiff Joints			
14C	26000	20.89	72.8	1315	72.8	126.0
14D	14000	33.89	23.5	690	67.1	116.2
14B	19000	40.39	26.6	930	85.0	147.3

[a] All length dimensions in Å units.

Dilute Solutions. In Table I are presented the R_G values calculated for the zigzag polyamides from their measured M_w and known l_o, N, and L_w. Two models were used: the classical Gaussian with freely jointed coils and the modified coils where the chains are freely rotating. It should be borne in mind, however, that the stiff joint zigzag polyamides are supposed to possess even larger R_G by virtue of having joints with significantly reduced freedom of torsional rotation. In Table II radii derived from diffusion and viscosity measurements are presented. As is expected from theory,[28] the measured R_H is consistently smaller than R_{Gvisc}. Naturally, R_{Gfd} is larger than R_{Gnd}. The point to note in Table II is that R_{Gnd} and R_{Gvisc} for each of the six polyamides are extremely close. The excellent agreement between thse two radii reflects, we believe, a high level of precission in the determinations of M_w, $[\eta]$, and R_H.

Radii of gyration obtained by diffusion-independent light scattering technique, that is, R_{Gdep}, are presented with the relevant parameters in Table III. Among these, the persistence lengths, q, are especially noteworthy. Most importantly, the R_{Gdep} values in Table III are much larger than the corresponding R_{Gvisc} and R_{Gnd} in Table II.

We conclude, therefore, that for each of the six zigzag polyamides, two kinds of R_G were measured. One is a consistently small R_G, namely, R_{Gvisc} or R_{Gnd}, which is only somewhat larger than R_H and is of the same order of magnitude as R_{Gg}. These measured radii all reflect hydrodynamic and thermodynamic interactions between the polymeric coils and solvent molecules in dilute solution. The second kind of R_G's, such as R_{Gdep}, do not reflect

Table II
Radii of Gyration from Diffusion-Related Measurements[a]

polymer code	$[\eta]$	M_w	l_o	m_o	N	L_w	R_H	R_{Gvisc}	R_{Gnd}	R_{Gfd}	10^7D, cm^2/s
					Freely Rotating Joints						
1a	0.98	24000	10.64	211	114	1050	59	84.2	79.9	145.2	1.55
1b	0.76	18000	17.14	330	55	810	45	70.3	69.8	126.8	2.03
1c	0.90	22000	23.64	449	49	1000	52	79.5	78.1	141.9	1.76
					Stiff Joints						
14C	0.80	26000	20.89	357	72.8	1315	54	80.8	78.6	142.8	1.69
14D	0.49	14000	33.89	595	23.5	690	43	55.9	48.4	87.9	2.125
14B	0.51	19000	40.39	714	26.6	930	47	62.7	60.1	109.2	1.94

[a] Intrinsic viscosities in dL/g. All dimensions in Å units.

Table III
Radii of Gyration Determined by Depolarized Light Scattering[a]

polymer code	M_w	l_o	N	L_w	depolarization ratio			R_{Gdep}
					δ_o^2	Δ^2	q	
				Freely Rotating Joints				
1a	24000	10.64	114	1050	0.69	0.0396	93.1	159.1
1b	18000	17.14	55	810	0.69	0.040	72.6	123.2
1c	22000	23.64	49	1000	0.69	0.040	89.6	152.2
				Stiff Joints				
14C	26000	20.89	72.8	1315	0.69	0.031	90.7	180.5
14D	14000	33.89	23.5	690	0.69	0.0667	105.4	126.5
14B	19000	40.39	26.6	930	0.69	0.095	207.5	190.4

[a] All lengths in Å units. All measurements at 25 °C in DMAc/5% LiCl. δ_o^2 extrapolated from Δ^2 of polymers, oligomers,[19] and benzanilide ($\Delta^2 = 0.63$).

Table IV
$R_H/M_w^{1/2}$ and $R_G/M_w^{1/2}$ for Zigzag Polyamides[a]

polymer code	M_w	l_o	$R_H/M_w^{1/2}$	$R_{Gvisc}/M_w^{1/2}$	$R_{Gnd}/M_w^{1/2}$	$R_{Gfd}/M_w^{1/2}$	$R_{Gg}/M_w^{1/2}$	$R_{Gfr}/M_w^{1/2}$	$R_{Gdep}/M_w^{1/2}$
					Freely Rotating Joints				
1a	24000	10.64	0.381	0.544	0.516	0.937	0.300	0.508	1.027
1b	18000	17.14	0.335	0.524	0.520	0.945	0.387	0.670	0.918
1c	22000	23.64	0.351	0.536	0.527	0.957	0.456	0.789	1.026
					Stiff Joints				
14C	26000	20.89	0.335	0.501	0.487	0.886	0.451	0.781	1.119
14D	14000	33.89	0.363	0.472	0.409	0.743	0.567	0.982	1.069
14B	19000	40.39	0.341	0.455	0.436	0.792	0.617	1.069	1.381

[a] Distances in Å units.

interactions with the solvent but the inherent size of the polymeric coil itself and are much larger than the smaller R_G's.

A qualitative measure of the polymeric coil's expansion can be gathered from the ratios of R_G to $M_w^{1/2}$. These are tabulated together with $R_H/M_w^{1/2}$ in Table IV. Several experimental results and one theoretical are plotted in Figure 1 against the length l_o of the rodlike segments. As expected, a strong dependence of $R_{Gdep}/M_w^{1/2}$ on l_o is clearly evident. It is obvious that R_H and R_{Gvisc} are completely independent from l_o.

In our intrinsic viscosity measurements it was observed that plots of $(\eta_o - \eta_s)/\eta_s c$ against c, over the concentration range of $0.125 < c < 0.500\%$, show a very small slope. We therefore believe that our values of R_{Gvisc} are close approximations of their values at the unperturbed state. This is corroborated by the small values of the second virial coefficients, all in the range of $19 \times 10^{-4} < A_2 < 49 \times 10^{-4}$ mol·mL/g^2, obtained for our modest molecular weight polyamides in light scattering experiments. By extension, the other R_G's reported above are also assumed to approximate unperturbed sizes. A comparison is, thus, valid of our $R_{Gvisc}/M_w^{1/2}$, in Table IV, with literature values of $R_{Gvisc}/M_w^{1/2}$ presented in *Polymer Handbook*[29] in terms of unperturbed chain end-to-end distance and with the values for rigid extended chains.[17,30] Literature values of $R_{Gvisc}/M_w^{1/2}$ of several polymers representing varying degrees of coil expansion are presented in Table V together with the corresponding sizes of l_o taken from previous tabulation by this author.[31] The comparison clearly shows that the zigzag polyamide coils are substantially more expanded than the coils of common flexible polymers and of derivatized cellulose. In should be noted that $R_{Gvisc}/M_w^{1/2}$ of the freely rotating zigzag polymers are consistently larger than the $R_{Gvisc}/M_w^{1/2}$ of the stiff joints polyamides, reflecting a lower solvent retention ability of the latter.

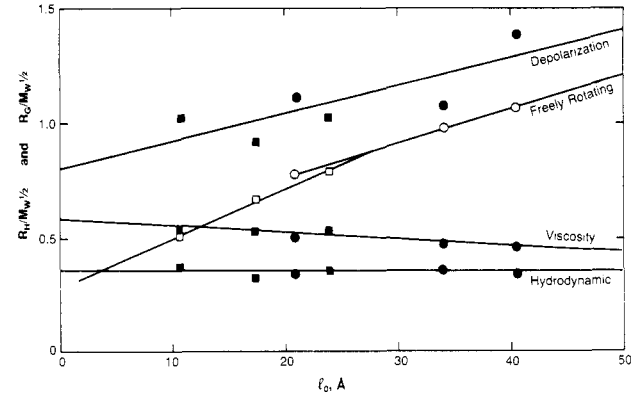

Figure 1. $R_H/M_w^{1/2}$ and $R_G/M_w^{1/2}$ as function of the length l_o: □, freely rotating joints; ○,●, stiff joints; full symbols, experimental; empty symbols, theoretical.

Table V
Literature Values of $R_{Gvisc}/M_w^{1/2}$ for Typical Polymers

polymer	l_o, Å	$R_{Gvisc}/M_w^{1/2}$, Å
poly(dimethylsiloxane)	1.46	0.270
poly(methyl methacrylate)	1.54	0.245 ± 0.01
poly(vinyl acetate)	1.54	0.295 ± 0.025
polystyrene	1.54	0.275
poly(ethylene terephthalate)	2.14	0.370
poly(2,6-dimethyl-1,4-phenylene oxide)	5.41	0.345
cellulose triacetate	7.75	0.300 ± 0.002
(hydroxyethyl)cellulose	7.75	0.408
poly(*p*-benzamide) in DMAc/LiCl	12.0	1.126 ± 0.124
poly(*p*-phenylene terephthalamide) in H_2SO_4	12.0	1.755 ± 0.043
poly(*p*-benzamide) in H_2SO_4	12.0	2.033

Table VI
Radii Ratios of Zigzag Polyamides[a]

polymer code	R_H/R_{Gvisc}	R_H/R_{Gnd}	R_H/R_{Gfd}	R_H/R_{Gfr}	R_H/R_{Gdep}
			Freely Rotating Joints		
1a	0.700	0.739	0.406	0.750	0.371
1b	0.640	0.645	0.355	0.501	0.365
1c	0.654	0.666	0.366	0.444	0.342
			Stiff Joints		
14C	0.668	0.687	0.378	0.429	0.299
14D	0.769	0.888	0.489	0.370	0.340
14B	0.750	0.782	0.430	0.319	0.247

[a] Radii ratios are identical with $(R_H/M_w^{1/2})/(R_G/M_w^{1/2})$ ratios.

Another measure of coil expansion are the R_H/R_{Gfr} ratios. These, and other R_H/R_G values, are tabulated in Table VI. The largest R_H/R_{Gfr} ratio is 0.750 for polymer **1a** while all other polymers are characterized by R_H/R_{Gfr} ratios substantially smaller than 0.54. This last value was calculated[32,33] to be the smallest possible for the fully swollen, freely jointed Gaussian chain model. The small R_H/R_{Gfr} ratios indicate that the zigzag polyamides, with the possible but improbable exception of **1a**, are not conventional Gaussian coils but are more expanded coils. The very small values of R_H/R_{Gfr} for the stiff joints zigzag polymers indicate these to be more expanded than their freely rotatingt analogs. The decrease in R_H/R_{Gfr} with increase in l_o within each family reflects the increase in coil expansion with increase in l_o, as expected. Similar indications of coil openness can be obtained from the ratios R_{Gvisc}/R_{Gfr} or R_{Gvisc}/R_{Gdep} where the smaller the ratio the more expanded the coil is. A plot of R_{Gvisc}/R_{Gfr} against l_o, in Figure 2, clearly shows that the polymeric coils become more open as l_o increases. For R_G's reflecting solvent entrainment, the ratios R_H/R_{Gvisc} and R_H/R_{Gnd} all fall in the interval of 0.640–0.888, spanning the ratios expected for normal flexible polymer coils.[28]

The above results indicate that the zigzag polyamides can be envisioned as rather expanded coils, with polymers having large l_o being more expanded than members of the same family with smaller l_o and with the stiffly jointed ones being somewhat more open than the freely rotating polymers. The small R_H, R_{Gvisc}, and R_{Gnd}, as compared with the much larger R_{Gdep} and R_{Gfd}, reflect, we believe, the volume of solvent entrained by the chain and idealized as a sphere of rather small radius. Using R_H as an example, we calculate from the corresponding volume V_H of the equivalent hydrodynamic sphere and the contour length Nl_o of the polymer chain, the cross sectional area of the cylindrical solvent envelop associated with each chain, as well as the diameter, d, of each such envelop. The results are given in Table VII. Recalling that the diameter of a naked polyamide chain is around 6 Å, we find that the thickness of the solvent layer around it is between about 8.5 and 12 Å; that is, two to three solvent molecules deep. A schematic representation of the system with a hypothetical chain of $N = 83$ and $l_o = 20$ Å is shown in Figure 3. The sizes of R_H and R_{Gfr} are shown together with the representative chain for clarity.

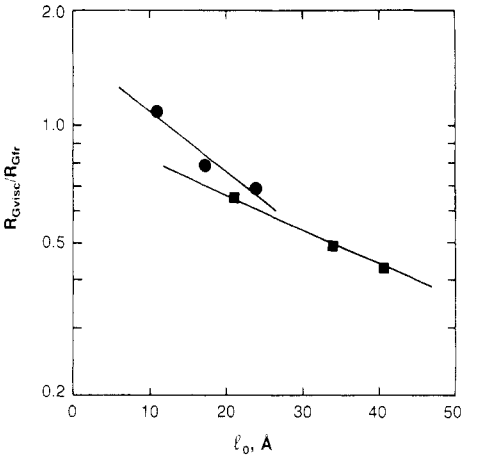

Figure 2. R_{Gvisc}/R_{Gfr} as function of l_o: ●, freely rotating joints; ■, stiff joints.

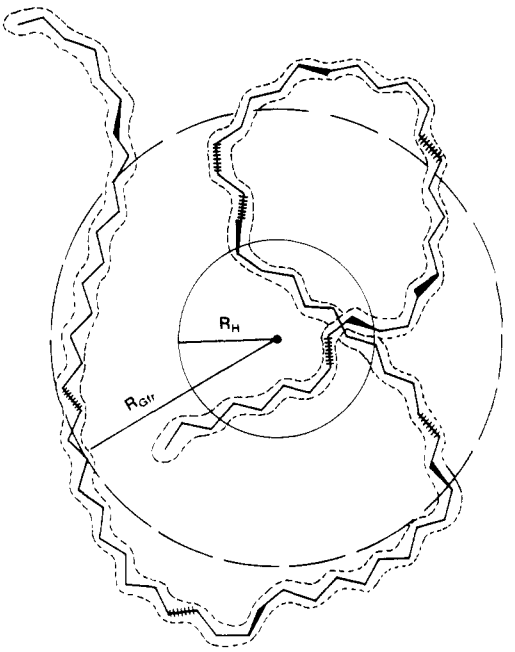

Figure 3. Schematic representation of a zigzag polyamide chain with $N = 83$, $l_o = 20$ Å, $R_H = 60$ Å, and $R_{Gfr} = 130$ Å. Dotted line represents the approximate boundary of the entrained solvent layer.

Table VII
Diameters of Solvated Zigzag Polyamide Chains from Hydrodynamic Radius

polymer code	R_H, Å	V_H, Å^3	Nl_o, Å	V_H/Nl_o, Å^2	d, Å
1a	59	859 853	1213.0	708.9	30.0
1b	45	381 510	942.7	404.7	22.8
1c	52	588 679	1158.4	508.2	25.4
14C	54	659 249	1520.8	433.5	23.4
14D	43	332 869	796.4	418.0	23.1
14B	47	434 672	1074.4	404.6	22.7

Concentrated Solution. A critical concentration, C^*, at which coil overlap first occurs uniformly throughout a polymer solution may be obtained from

$$C^* = M_w/R_{Gvisc}{}^3 N_a \quad (15a)$$

or[27]

$$C^* = 0.64/[\eta] \quad (15b)$$

Table VIII
Solution Viscosities of Zigzag Polyamides[a]

freely rotating joints, η_0 in cP				stiff joints, η_0 in cP			
	polymer				polymer		
concn, %	1a	1b	1c	concn, %	14C	14D	14B
25.0			20000	25.0		34000	53000
15.0	1745.0	1390.0	1945.0	15.0	1336.0	2910.0	3500
13.0	1100.0	740.0	1120.0	13.75		1700.0	
11.0	600.0	385.0	520.0	12.0	609.0	910.0	986.0
10.0	431.8	238.1	312.6	11.0		632.0	710.0
8.33	210.7	122.8	157.3	10.0	294.0	370.0	400.0
6.94	118.2	73.2	89.8	7.5	120.0	118.2	130.0
5.95	77.9	50.0	59.2	5.0	52.7	48.2	50.5
5.21	55.3	36.7	42.9	2.0	12.0	10.4	11.1
4.17	33.9	23.6	26.8	1.0	7.73	6.91	7.27
3.2	21.3	15.3	17.0	0.5	3.47	3.06	3.01
2.6	15.4	11.4	12.4	0.33	3.08	2.82	2.80
1.98	10.9	8.3	9.0	0.25	2.90	2.71	2.71
1.02	5.1	4.8	5.8	0.125	2.65	2.55	2.55
0.51	3.86	3.49	3.52				
0.34	3.36	3.14	3.11				
0.26	3.12	2.95	2.92				
0.128	2.76	2.68	2.64				
C^*	0.668	0.861	0.727	C^*	0.819	1.331	1.280

[a] All measurements in DMAc/5% LiCl at 25.0 °C. Solvent viscosity is 2.39 cP. Values of C^* are in wt/v %.

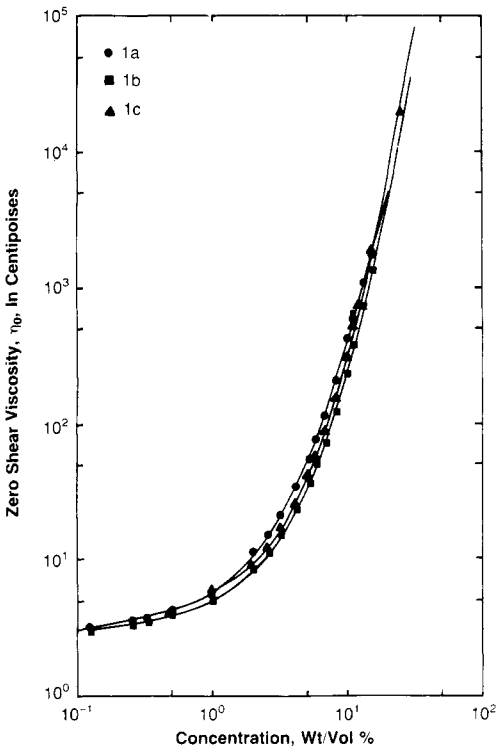

Figure 4. Viscosity of freely rotating zigzag polyamides in DMAc/5% LiCl at 25 °C.

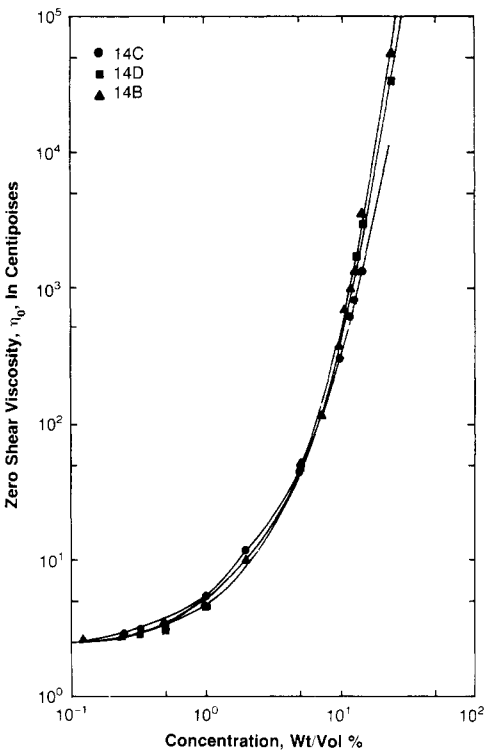

Figure 5. Viscosity of stiff joints zigzag polyamides in DMAc/5% LiCl at 25 °C.

obtainable from eq 15a by the use of eq 12 above. It should be noted that the exact size of the numerator in eq 15a depends on Flory's universal parameter ϕ_∞ and will change slightly with changes in ϕ_∞. Using the data in Table II, the values of C^* for the six zigzag polyamides were calculated according to eq 15a. They are listed in Table VIII together with the viscosities of the polymers in solutions up to 25 wt/v % concentration for polymers **1c**, **14D**, and **14B** and 15 wt/v % for the others. For clarity, the viscosities are plotted against concentration in log–log scale in Figures 4 and 5. A break at C^* is observed in neither curve, but a smooth increase in the slope of all curves does become evident around C^*. This concentration region is substantially lower than the critical concentration for entanglement, C_c, usually defined as the point of intersection of the straight lines tangential to the low and high concentration branches of the viscosity curve. In our case C_c appears at concentrations of ~2.5 to ~3.5%, resulting in $M_c = (M_w C_c)$ of around 500. This is a very low value for M_c, corresponding to the molecular weight of only one or two rodlike segments. It reflects substantially open coils and deep molecular interpenetration already at these modest concentrations. As is obvious from Figures 4 and 5, at higher concentrations increasing levels of interpenetration and intermolecular entanglements continuously increase the slope of the viscosity vs concentration curves. When plotted on log–log scale, the η_0 vs c curves are linear at concentrations over 10%. As is evident from Figures

Table IX
Concentration Dependence of η_0 at $c > 10\%$[a]

polymer code	m_w	l_o, Å	points considered at $10 \leq c \leq 15\%$	correlatn param, r	K_1 in eq 16	a in eq 16	η_0 at 15% concn	$100\ \eta_0/M_w$
				Freely Rotating Joints				
1a	24000	10.64	4	0.9997	1.266×10^6	3.47	1745	7.27
1b	18000	17.14	4	0.9992	4.644×10^6	4.28	1390	7.72
1c	22000	23.64	5	0.9985	9.952×10^6	4.48	1945	8.84
				Stiff Joints				
14C	26000	20.89	4	0.9994	1.607×10^6	3.73	1336	5.14
14D	14000	33.89	7	0.9979	3.059×10^7	4.91	2910	20.79
14B	19000	40.39	6	0.9980	8.562×10^7	5.33	3500	18.42

[a] Viscosities in cP.

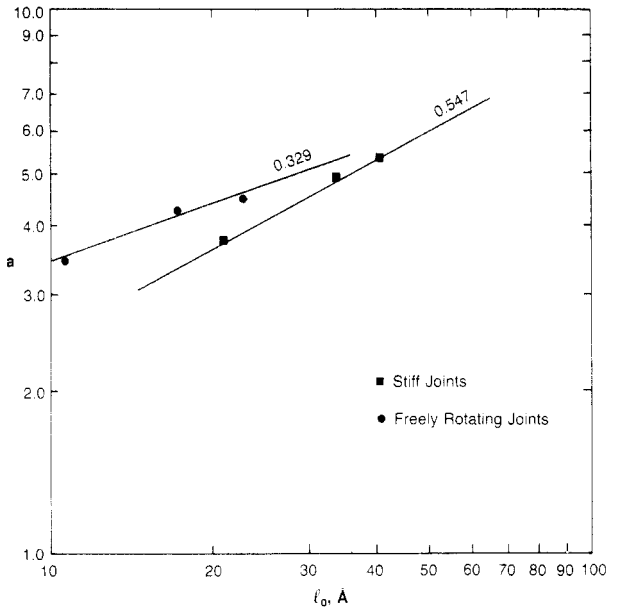

Figure 6. High concentration power dependency of the viscosity vs concentration on length l_o of rodlike segments of freely rotating (●) and stiff (■) joints zigzag polyamides.

4 and 5, but far clearer from a statistical analysis of all the data points in this concentration regime, the slopes of the curves for the stiff joints polyamides are higher than those for the freely rotating polymers, and the larger is l_o within each family the steeper is the slope. The numerical data are listed in Table IX. The slopes which are the exponents a in the equation

$$\eta_o = K_1 c^a \tag{16}$$

are plotted in Figure 6 in double logarithmic scale against the rodlike segment length l_o. The data fall on two straight lines described by the equality

$$a = K_2 l_o^b \tag{17}$$

where for the freely rotating joints zigzag polyamides

$$a = 1.618 l_o^{0.329} \qquad r = 0.9705$$

and for the stiff joints zigzag polyamides

$$a = 0.709 l_o^{0.547} \qquad r = 0.9993$$

Above $c = 10\%$ the polymers are deeply in the concentrated solution regime. The results in Tables VIII and IX and Figures 4–6 clearly indicate that in this regime the polymer solution viscosity depends on both the flexibility of the joints between rodlike segments and their length l_o. Furthermore, when measured at 10% concentration, the viscosity shows a dependence on M_w and l_o, but when measured at 15% and higher, the dependence of the viscosity on l_o dominates and no obvious dependence on M_w is noticed. The ratios η_0/M_w at 15% clearly increase with l_o and their very large values for the large l_o stiff joints polyamides reflect, we believe, the large expansion of their polymeric coils.

Table X
Crystallinity Indices and Densities of Zigzag Polyamides

polymer code	% crystallinity	D, g/cm^3
	Freely Rotating Joints	
1a	48	1.357
1b	50	1.359
1c	44	1.371
	Stiff Joints	
14C	38	1.338
14D	25	1.310
14B	25	1.317

Solutions in concentrations up to 40 wt/wt % in DMAc/5% LiCl were prepared from all polyamides in this study. All solutions were isotropic in the quiescent state, and no stir opalescence could be induced in them. The solutions were all slow flowing and fully transparent and maintained their appearance and behavior for at least 1 year at ambient temperature. This indicates the solutions not to be transparent gels and that no optical scale phase separation existed in them or formed with time. Depending on the particular polyamide, at higher than 35–40% concentration, swollen polymeric gel particles appeared in amounts and size that increased with concentration. The above behavior of the zigzag polyamides is unlike that of rodlike polyamides, such as poly(*p*-benzamide) and poly(*p*-phenylene terephthalamide), which exhibit lyotropic liquid crystallinity in the same solvent system at concentrations of 7% or less as is well-documented in the literature.[14,34-36]

The viscosities of the zigzag polyamides in the concentrated solution regime are far higher than those of flexible polymers of comparable molecular weights and concentrations. For example, an 11 wt/vol % solution of poly(ε-caprolactam) of $M_w = 42500$ in formic acid, in which viscosity-enhancing hydrogen-bond interactions are abundant, has a viscosity very close to 70 cP.[37] This viscosity is 1–2 orders of magnitude smaller than the viscosities at 10% concentration of the zigzag polyamides of much lower molecular weight.

Bulk. The results of bulk density measurements are tabulated in Table X together with the crystallinity indices estimated from WAXD patterns. The densities fall in the range generally observed for aromatic polyamides,[1,38] and the slight drop in density of the stiff joints zigzag polyamides reflects their lower crystallinity as compared with the freely rotating polyamides. The reduced crystallinity

of the stiff joints polyamides reflects, we believe, the possibility that it is harder for these molecules than for the freely rotating ones to pack in register and develop crystallinity.

Discussion

When considered together, the dilute solution properties of the six zigzag polyamides indicate them to be substantially coiled and definitely not extended in space in the shape of a planar zigzag in which all bonds are in their trans conformation. Most instructive are the absolute values of the intrinsic viscosity that are about 1 order of magnitude smaller than the values for rodlike aromatic polyamides of similar chemical structure and comparable molecular weights.[17,39,40] The very slow increase of the reduced viscosity $[(\eta_o - \eta_s)/\eta_s c]$ with concentration c in the dilute solution regime is, again, an indication that our polyamides do not behave as elongated stiff particles but more so as coils. These may be generally spherical or in the shape of ellipsoids of revolution where the large semiaxis is not very large relative to the minor semiaxis. At the same time, the values of R_{Gdis} and R_{Gdep} as well as $R_{Gvisc}/M_w^{1/2}$ all indicate that the zigzag polyamide coils are substantially more expanded in space than coils of conventional flexible polymers. The above data indicate that this expansion is due to the length of the rodlike segments in the zigzag polyamides, each behaving as a single statistical bond of length l_o. Because of the similar angles between rigid segments all the zigzag polyamides are characterized by an R_{Gfr} very close to $1.7R_{Gg}$. A comparison of the data in Tables I and III reveals that R_{Gdep} is somewhat larger than the calculated R_{Gfr}. This indicates that in dilute solution the zigzag polyamides adopt a spatial configuration dictated by their equilibrium rigidity and that the kinetic rigidity is not noticeable. The lack of sensitivity to kinetic effects is clearly visible in Figures 4 and 5, where the viscosity of all polymers in the dilute solution regime shows a remarkably similar dependence on concentration and independence from the length l_o of the rodlike segments and the stiffness of the joints between them.

The dramatic difference between the rather large R_{Gdep}, obtained by a light scattering technique insensitive to hydrodynamic interactions with solvent molecules, and the far smaller R_G's sensitive to such interactions, such as R_{Gvisc}, R_{Gfd}, R_{Gnd}, and, especially, the hydrodynamic radius R_H, clearly indicates that the measured radii do not arise from the same cause. Indeed, we believe that R_{Gdep} describes the polymeric coil alone, with solvent effects being small and secondary at most. On the other hand, R_H, R_{Gisc}, etc. are measures of idealized equivalent spheres, each containing both the volume of the naked polymeric chain and the entrained solvent molecules. Combining both kinds of measurements we arrive at the schematic representation in Figure 3, according to which the chains with large l_o exist in solution as substatially expanded coils. The polymer chains are encased in a dynamic sheath of solvent molecules the thickness of which is about two to three solvent molecules thick. As the polymer coil moves in solution, the solvent molecules comprising the sheath move with it such that the combined volume of the polymeric chain and the solvent sheath equals the volme of the equivalent hydrodynamic sphere. Following Tanford[28] it is easily shown that the other diffusion-related radii (R_{Gvisc}, R_{Gnd}, and R_{Gfd}) are all related to R_H and, hence, explained by the above model.

As we move into the concentrated solution regime, an increasing dependence of the viscosity on both joint stiffness and segmental length become clearly evident, as can be gathered from Tables VIII and IX and Figures 4–6. The results in Figure 6 are especially interesting as they clearly show the difference in the increase of the viscosity with l_o between the freely rotating and the stiff jointed groups. The higher power dependence shown in Figure 6 and the consistently higher viscosities of the stiffer polymers of comparable l_o's as compared with the freely rotating ones at the same concentration reflect the effects of kinetic rigidity superimposed on those associated with the equilibrium rigidity.

At the high concentration regime, the increases in the viscosity with l_o reflect the fact that as l_o becomes longer, the rodlike segments each sweeps larger volume upon interconverting from one rotational isomeric position to another. With the increased volume swept a commensurate increase in the interference to the mobility and rotation of other segments, and chains, ensues. The higher power dependence of the viscosity increase exhibited by the stiffly jointed polyamides reflects the fact that in their case the change from one rotational isomeric state to another is substantially slower, resulting in higher interference to the motion of other segments and coils than in the case of the freely rotating zigzag polyamides. In the dilute solution where each polymeric coil is separated from others, the rate of conversion from one isomeric state to another does not affect other coils and hence the independence of their solution behavior from kinetic rigidity.

The reduced crystallinity of the stiff jointed polyamides, in Table X, also reflects, we believe, kinetic rigidity effects, slowing the torsional rotation of segments in space and reducing their ability to pack well in register and crystallize. This observation is especially valid in light of the fact that it holds for polyamides of comparable l_o and because all the zigzag polyamides have about the same frequency of amide groups along their backbone. Infrared scans showed that in all polyamides essentially all the amide groups are hydrogen bonded, independently of the level of crystallinity.

The inability of the zigzag polyamides to form liquid crystalline solutions reflects a low capability for parallel packing of the rodlike segments in volumes sufficiently large to produce liquid crystalline domains. This poor packing ability is more acute in the case of the stiff joints polymers as is apparent from the lower crystallinity indices of the bulk polyamides. The poor packing ability and the absence of lyotropic mesomorphicity stand in dramatic contradistinction to the rodlike aromatic polyamides reported in the literature.[14,34,35,36]

Acknowledgment. The help of Drs. K. Zero and W. B. Hammond with light scattering and NMR spectroscopy measurements is gratefully acknowledged. The author thanks Professor Sir Sam Edwards for many fruitful discussions.

Registry No. **1a** (copolymer), 28853-54-5; **1a** (SRU), 26854-94-4; **1b** (copolymer), 28853-50-1; **1b** (SRU), 31868-46-9; **1c** (copolymer), 111159-60-5; (4,4′-diaminobenzanilide)(*p*-dicarboxyphenylene isophthalamide), 111159-62-7; (4,4′-diaminobenzanilide isophthalamide)(terephthalic acid) (copolymer), 111189-10-7; (4,4′-diaminobenzanilide)(isophthalic acid) (copolymer), 29155-99-5.

References and Notes

(1) Aharoni, S. M. *Macromolecules* **1987**, *20*, 877.
(2) Vitovskaya, M. G.; Astapenko, E. P.; Nikolayev, V. Ya.; Didenko, S. A.; Tsvetkov, V. N. *Polym. Sci. USSR (Engl. Transl.)* **1976**, *18*, 788.
(3) Tsvetkov, V. N. *Polym. Sci. USSR (Engl. Transl.)* **1979**, *21*, 2879.
(4) Tsvetkov, V. N. *Polym. Sci. USSR (Engl. Transl.)* **1977**, *19*, 2485.

(5) Tsvetkov, V. N.; Andreeva, L. N. *Adv. Polym. Sci.* **1981**, *39*, 95.
(6) Bishop, M. T.; Karasz, F. E.; Russo, P. S.; Langley, K. H. *Macromolecules* **1985**, *18*, 86.
(7) Shtennikova, I. N.; Peker, T. V.; Garmonova, T. I.; Mikhailova, N. A. *Eur. Polym. J.* **1984**, *20*, 1003.
(8) Nekrasov, I. K. *Polym. Sci. USSR (Engl. Trans.)* **1971**, *13*, 1920.
(9) Aharoni, S. M. *Macromolecules* **1986**, *19*, 426.
(10) Khazaryan, L. G.; Tsvankin, D. Ya.; Vasilev, V. A.; Dakhis, M. A.; Tolkachev, Yu. A. *Polym. Sci. USSR* **1975**, *17*, 1797.
(11) Dawson, P. C.; Blundell, D. J. *Polymer* **1980**, *21*, 577.
(12) Aharoni, S. M.; Sharma, R. K.; Szobota, J. S.; Vernick, D. A. *J. Appl. Polym. Sci.* **1983**, *28*, 2177.
(13) Yamazaki, N.; Matsumoto, M.; Higashi, F. *J. Polym. Sci., Polym. Chem. Ed.* **1975**, *13*, 1373.
(14) Aharoni, S. M. *J. Appl. Polym. Sci.* **1980**, *25*, 2891.
(15) Benoit, H.; Doty, P. M. *J. Phys. Chem.* **1953**, *57*, 958.
(16) Arpin, M.; Strazielle, C.; Weill, G.; Benoit, H. *Polymer* **1977**, *18*, 262.
(17) Arpin, M.; Strazielle, C. *Polymer* **1977**, *18*, 591.
(18) Kerker, M. *The Scattering of Light and Other Electromagnetic Radiation*; Academic: New York, 1969; Chapter 10, pp 574-619.
(19) Zero, K.; Aharoni, S. M. *Macromolecules* **1987**, *20*, 1957.
(20) Tonelli, A. E. *Macromolecules* **1972**, *5*, 558.
(21) Tonelli, A. E. *Macromolecules* **1973**, *6*, 503.
(22) Hummel, J. P.; Flory, P. J. *Macromolecules* **1980**, *13*, 479.
(23) Erman, B.; Flory, P. J.; Hummel, J. P. *Macromolecules* **1980**, *13*, 484.
(24) Flory, P. J. *Principles of Polymer Chemistry*; Cornell University: Ithaca, NY, 1953 Chapters X and XIV.
(25) Yamakawa, H. *Modern Theory of Polymer Solutions*; Harper & Row: New York, 1971; pp 25, 56.
(26) Flory, P. J. *Statistical Mechanics of Chain Molecules*; Interscience: New York, 1969; Appendix G, pp 401-403.
(27) Graessley, W. W. *Adv. Polym. Sci.* **1974**, *16*, 1.
(28) Tanford, C. *Physical Chemistry of Macromolecules*; Wiley: New York, 1961; pp 138-179, 275-412.
(29) Kurata, M.; Tsunashima, Y.; Iwama, M.; Kamada, K. In *Polymer Handbook, Second Edition*; Brandrup, J., Immergut, E. H., Eds.; Wiley-Interscience: New York, 1975; p IV-1 ff.
(30) Millaud, B.; Strazielle, C. *Makromol. Chem.* **1978**, *179*, 1261.
(31) Aharoni, S. M. *Macromolecules* **1983**, *16*, 1722.
(32) Akcasu, A. Z.; Benmouna, M. *Macromolecules* **1978**, *11*, 1193.
(33) Huber, K.; Burchard, W.; Akcasu, A. Z. *Macromolecules* **1985**, *18*, 2743.
(34) Morgan, P. W. *Macromolecules* **1977**, *10*, 1381 and patents cited therein.
(35) Kowlek, S. L.; Morgan, P. W.; Schaeffgen, J. R.; Gulrich, L. W. *Macromolecules* **1977**, *10*, 1390.
(36) Aharoni, S. M. *J. Polym. Sci., Polym. Phys. Ed.* **1981**, *19*, 281.
(37) Aharoni, S. M., unpublished results.
(38) Tashiro, K.; Kobayashi, M.; Tadokoro, H. *Macromolecules* **1977**, *10*, 413.
(39) Tsvetkov, V. N.; Kudriavtsev, G. I.; Shtennikova, I. N.; Peker, T. V.; Zakharova, E. N.; Kalmykova, V. D.; Volokhina, A. V. *Eur. Polym. J.* **1976**, *12*, 517.
(40) Tsvetkov, V. N.; Shtennikova, I. N.; Peker, T. V.; Kudriavtsev, G. I.; Volokhina, A. V.; Kalmykova, V. D. *Eur. Polym. J.* **1977**, *13*, 455.

Prediction of Polymer Crystal Structures and Properties. A Method Utilizing Simultaneous *Inter-* and *Intra*molecular Energy Minimization

R. A. Sorensen,† W. B. Liau, and R. H. Boyd*

Department of Chemical Engineering and Department of Materials Science and Engineering, University of Utah, Salt Lake City, Utah 84112. *Received May 18, 1987*

ABSTRACT: A method is described for using molecular mechanics to calculate in a unified manner, from transferable conformational energy functions, the packing parameters and energy, vibrational dispersion curves, heat capacity and thermodynamic functions, elastic constants, and refractive indices of polymer crystals. The *inter-* and *intra*molecular conformational energies are simultaneously minimized. This allows assessment of the effect of packing forces on the polymer helix parameters and the intramolecular geometry. In addition, the converged Newton-Raphson coefficient matrix used in minimization allows convenient vibrational analysis and calculation of the elastic constants of the crystal.

Molecular mechanics calculations have proven very useful in accounting for the conformational energetics and properties of polymer molecules. The method is based on the premise that a molecule can be simulated by empirical transferable energy functions that represent bond stretching, bending, and twisting as well as more distant nonbonded or steric interactions. Electrostatic forces are included when appropriate. Stable conformations are found as minima in the total energy function. When applied to a segment of an isolated polymer molecule, the most stable local conformation, when repeated, often can be indentified as the conformation of the helix obtaining in the crystalline state. The molecular mechanics calculations on a variety of local conformations often can be summarized by association of local conformations with structurally motivated energy parameters (e.g., gauche trans energy differences, four-bond pentane interferences, etc.). These parameters then lead to statistical weight matrices that may be utilized as input to statistical calculations of the average properties of disordered long chains.[1] This process has reached a high state of development and had many successes. In bulk systems, defects and energy paths for molecular motion in polymer crystals have been successfully described via conformational energy calculations.[2-4]

There has also been interest in predicting the packing and structure of polymer crystals.[5,6] It is this subject that is the concern of the present work. Most past effort in this area has proceeded via a reasonable two-step process. A conformation of the polymer helix is adopted. It is determined either from molecular mechanics calculations on the isolated molecule or from other sources. Then the packing is analyzed by assembling the polymer helices, assuming no further change in conformation. Thus, *inter*molecular nonbonded and polar energy functions are the only participants in the total energy function optimized. In the present work we generalize the packing analysis by describing a method where both the *intra*molecular and intermolecular degrees of freedom are permitted to participate simultaneously in the optimization. The motivation for this is twofold. First, although the rigid molecule analysis is no doubt viable in numerous cases, there are also important ones known where there

†Present address: Systems Technology Division, IBM Corp., Austin, TX 78758.

0024-9297/88/2221-0194$01.50/0